

Structure and Activity of NiCo–Mo/SiO₂ Hydrodesulfurization Catalysts

JORGE LAINE, JOAQUÍN L. BRITO, AND FRANCISCO SEVERINO

*Laboratorio de Físico-Química de Superficies, Instituto Venezolano de Investigaciones Científicas,
Apt. 21827, Caracas 1020-A, Venezuela*

Received December 11, 1990; revised May 11, 1991

A series of Ni–Co–Mo hydrodesulfurization (HDS) catalysts supported on silica was prepared varying the ratio $r = \text{Co}/(\text{Co} + \text{Ni})$ between 0 and 1, maintaining Mo and (Co + Ni) concentrations constant. Calcination temperatures employed were 500 and 600°C. The promoter (Co and/or Ni) was present in the precursor as a hydrated molybdate phase that suppressed both anhydrous MoO₃ crystallite growth and decrease in surface area resulting from sintering of the support. Both phenomena occurred in the nonpromoted catalyst after calcining at 600°C, probably by a dehydroxylation process resulting from dislinking of polymolybdates from the silica support. A correlation between TPR and dispersion given by XRD was established, confirming that the dispersion of molybdenum on silica was lower than that on the aluminas previously studied. According to the proposed correlation, sulfidation caused an increase in dispersion in all the catalysts. The presence of anhydrous MoO₃ was held responsible for the formation of amorphous MoO₂ observed by TPR after sulfidation. The increase in dispersion after sulfidation was accompanied by a remarkable increase in the initial HDS activity of both nonpromoted and promoted catalysts. However, the nonpromoted sample showed a pronounced initial deactivation during use. Compared with another similar, but supported on alumina, series of catalysts, a minimum instead of a maximum steady-state HDS activity was found for an intermediate value of r . © 1991 Academic Press, Inc.

INTRODUCTION

The role of promoters (Co or Ni) in HDS catalysts has been the objective of considerable debate. Most approaches have advocated structural aspects (1–5). The two main theories assume that the active catalyst state is either a single phase, i.e., the promoter incorporated in MoS₂ (6), or biphasic, i.e., Co₈S₉ + MoS₂ (7). The edge plane in MoS₂ crystallites has been suggested to be more active than the basal plane (8, 9), and the HDS activity has been related to the number of promoter atoms located at the edges (10). The promotion seems to be associated with a donation of electrons from the promoter to Mo (11). Other authors (12–14) have pointed out that the promoter can exhibit a high activity even by itself, and thus the synergistic effect of the promoter on Mo can be interpreted in terms of additivity of the MoS₂ and

the promoter activities. Other evidences have shown promoter effects related to inhibition of carbon deposition (15–17) and to maintenance of the dispersion of molybdenum sulfide (15). However, few works (18, 19) have been devoted to comparing Co and Ni as promoters of Mo catalysts.

The simultaneous presence of Co and Ni has been found to produce optima in the ratio $r = \text{Co}/(\text{Co} + \text{Ni})$ for higher HDS activity in series of molybdenum-based catalysts supported on alumina (20, 22). The optimum was found to be influenced by the method of catalyst preparation (20), in particular by the calcination temperature (21), i.e., r varied from ca. 0.3 to 0.7 when increasing calcination temperature from 500 to 600°C.

Since the presence of optima r -values has been proven with two aluminas of different origin (20), we were tempted to prepare sim-

ilar series of NiCoMo catalysts using a different support, silica, in order to investigate the dependency of the dual effect on the type of support. We were also aiming to complete more comprehensive information regarding the differences between Co and Ni as promoters of HDS catalysts.

EXPERIMENTAL

Catalysts were prepared by a two-step impregnation method. The support employed was a high-purity silica gel: Kieselgel 60 from Merck, 35–70 mesh, and surface area of 560 m²/g. This was first impregnated with enough ammonium heptamolybdate in aqueous solution to obtain a concentration of 10 wt% MoO₃. Volume of impregnating solution was slightly larger than the solid volume. Impregnation was carried out at 70°C stirring until the excess solvent was evaporated. The impregnated sample was dried in a forced convection oven at 120°C, and then calcined in a muffle furnace increasing temperature at 100°C/h to 500°C, at which it was left overnight. Portions of the resulting molybdate catalyst were coimpregnated with cobalt and (or) nickel in aqueous solutions of the nitrates using the appropriate concentration to obtain 3.0 wt% PO ($P = \text{Co} + \text{Ni}$). Impregnations were carried out as in the first step.

X-ray diffraction (XRD) spectra were carried out using CuK α radiation, Ni filter, and 40 kV. XRD signal broadening/sharpening was taken as a comparative measure for dispersion of the supported catalysts. Surface areas were measured employing a sorptometer apparatus using nitrogen adsorption at -196°C.

Temperature-programmed reduction (TPR) of the catalysts was carried out as described elsewhere (23). Briefly, the apparatus consisted of a flow system connected to a thermal conductivity cell to follow changes in the composition of the reducing gas (10 ml/min H₂ plus 40 ml/min N₂). The sample (100 mg) was placed into a tubular reactor which was heated at a constant rate (20°C/min). Water produced was removed with a liquid nitrogen trap at the outlet of

the reactor. Thus, the observed signal was related only to H₂ consumption. Presulfided samples (see procedure below) were cooled down in a stream of He before TPR.

The HDS activity of the catalyst was referred to thiophene conversion, which was measured in an atmospheric pressure continuous flow reactor connected to an on-line gas chromatograph. The reaction conditions were 100 ml/min H₂, 0.05 mol thiophene/mol H₂, and 400°C. Activity measurements on both presulfided (1 g) and nonpresulfided (2 g) catalyst samples were performed. For catalyst sulfiding, the sample was first treated at 300°C in H₂ for 1 h before H₂S admission and then sulfided with pure H₂S at 400°C for 2 h. This procedure has been found (24) to be an optimum presulfidation procedure. For activity tests on nonpresulfided samples, prior to reaction the catalyst was pretreated at 400°C in a helium flow for 1 h.

RESULTS

Surface Areas and Colors

The nonimpregnated silica, having originally 560 m²/g, suffered a decrease in surface area to 380 m²/g as a result of calcining at either 500 or 600°C.

Surface area did not vary significantly with either r -value or calcination temperature (T_c) in promoted catalysts (Fig. 1). However, an intermediate r -value seemed to give a minimum surface area.

In the case of the nonpromoted catalyst ($r = 0/0$ shown at the right-hand side of Fig. 1), surface area of the sample calcined at 500°C was about the same value as that of the calcined support; however, there was a remarkable decrease after calcining at 600°C.

Colors of calcined catalysts were as follows: pale green for $r = 0/0$, yellow for $r = 0$ turning to dark beige for intermediate r -values, and violet for Co-rich samples. These colors did not change significantly for the two T_c employed.

The yellow tone of sample with $r = 0$ is characteristic of hydrated nickel molybdate (25), a phase different from anhydrous

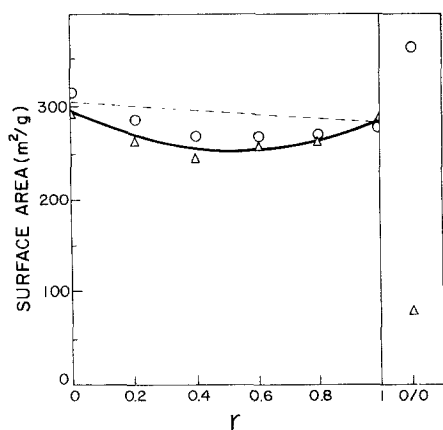


FIG. 1. Surface areas. Calcination at: O, 500°C; Δ, 600°C.

nickel molybdate (green). It is not possible to reach an analogous conclusion in the case of sample with $r = 1$, as both anhydrous and hydrated cobalt molybdates are known to have a similar violet tone.

X-Ray Diffraction

Supported molybdenum oxide produced small and broad peaks in the sample with $r = 0/0$ calcined at 500°C (Fig. 2A). However, it increased its crystallinity to form well-defined MoO₃ at $T_c = 600^\circ\text{C}$ (Fig. 2B). The small peak at $2\theta = 27.4^\circ$, which is present in most of the promoted samples and in the 0/0 samples calcined at 500°C and 600°C, has been found to be the most intense band in MoO₃ prepared by a continuous precipitation method (26), as opposed to the signal at $2\theta = 25.8^\circ$, which characterizes MoO₃ with preferential crystal growth in the (010) direction. The higher crystallinity of MoO₃ in the 0/0 sample calcined at 600°C is paralleled by a significant development of the 25.8° peak, but such an effect is absent in the case of promoted samples.

The increase in T_c also produced more definition of the broad background peak around $2\theta = 22^\circ$ corresponding to the silica support. Again, this effect seemed to occur only in the nonpromoted sample.

In addition to the $2\theta = 27.4^\circ$ peak, the promoted samples showed a larger signal

around $2\theta = 27^\circ$, assigned to the hydrated phase: $\text{PMoO}_4 \cdot n\text{H}_2\text{O}$ ($P = \text{Co}$ or Ni , JCPDS powder diffraction file N°-26-477 for Co and 13-128 for Ni). This signal was sharper at higher r -values ($r = 0.6-1$).

After sulfiding, XRD spectra (not shown) did not show peaks as in Fig. 2 but showed almost the same silica background spectrum in all cases, suggesting an increase in dispersion and/or deterioration of the crystalline order by sulfiding. Nevertheless, a very broad, not well-defined, small signal around $2\theta = 14^\circ$, probably corresponding to dispersed and/or defected MoS₂, was observed.

Temperature-Programmed Reduction

Figures 3 and 4 show TPR spectra of calcined and sulfided catalysts respectively.

Oxide samples showed a two-peak spectrum (Fig. 3), but transformed to a three-peak spectrum when increasing T_c from 500 to 600°C in the nonpromoted sample. This may be related to the formation of a highly crystalline MoO₃ after calcining at 600°C, as detected by XRD (Fig. 2B). The first peak (575°C) may be assigned to dispersed polymolybdates linked to the silica surface. Confirming this, Seyedmonir *et al.* (27) found by FTIR that polymolybdates are reduced in H₂ previously to free MoO₃. Accordingly, the second peak (655°C) in the nonpromoted sample calcined at 600°C can be assigned to bulk MoO₃. The peak located at the highest temperature is most likely due to poorly crystalline MoO₂ generated from the reduction of the MoO₃ phases.

In the case of promoted samples the shapes of TPR spectra are similar, and agree with that of the 0/0 catalyst calcined at 500°C, except for details in the sharpness and temperatures of peaks. This suggests that mixed phases in promoted samples have reducibility behavior similar to that of the polymolybdates and amorphous MoO₃ present in 0/0 calcined at 500°C.

After sulfiding, the spectrum of sample 0/0 calcined at 500°C was transformed almost exclusively to a unique, lower-temperature signal (Fig. 4A), which may be assigned to

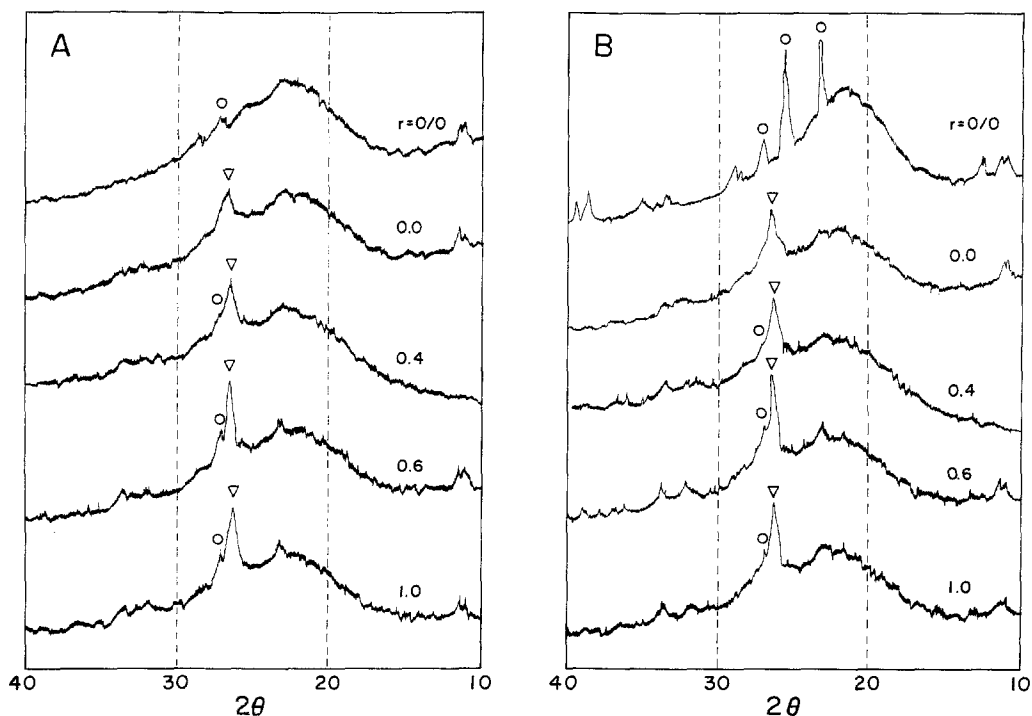


FIG. 2. XRD spectra of the oxide catalysts. Calcination at: (A) 500°C; (B) 600°C. Phases: ○, MoO_3 ; ▽, $\text{PMoO}_4 \cdot n\text{H}_2\text{O}$ ($P = \text{Ni}$ or Co).

well-dispersed molybdenum sulfide. However, a high-temperature signal, probably an oxidic phase (see Discussion), was detected after sulfiding sample 0/0 calcined at 600°C (Fig. 4B), suggesting that the appearance of such oxidic phase (probably MoO_2) impaired the sulfiding process.

Sulfided promoted samples showed two close low-temperature peaks in Ni-containing catalysts, but apparently showed only one in the Co-promoted sample. Also, Ni-rich samples displayed signals with broadening and asymmetry larger than those of the Co-rich samples.

In both oxidic (Fig. 3) and sulfided catalysts (Fig. 4) there was a decrease in the temperature of the first peak (i.e., an increase in initial reducibility) as r tended to 0.0. However, the sample with $r = 1.0$ seems to have had initial reducibility similar to the nonpromoted sample.

Catalytic Activity

Figure 5 shows HDS activity behavior of some selected samples calcined at 500°C.

The sulfided catalysts (Fig. 5a) showed an initial high activity followed by a progressive deactivation. The initial deactivation was significantly more pronounced in the case of the nonpromoted sample, although long-term deactivation (after about 2 h) appears to be the same.

Nonpresulfided samples (Fig. 5b) showed a rapid increase followed by a decrease in thiophene conversion (i.e., a peak in the activity behavior). This is most likely due to rapid thiophene consumption to accomplish catalyst sulfidation. Therefore, in this case the observed activity decay may not necessarily be a true deactivation but probably an effect related to the differences in kinetics between sulfidation and catalytic reaction. However, while the nonpromoted sample followed a slower and more pronounced activity decay after the peak (probably a true deactivation) the promoted catalysts showed more stable activities, and even slight activity increases, more clearly noticed in the high nickel content samples. A similar behavior was observed for samples

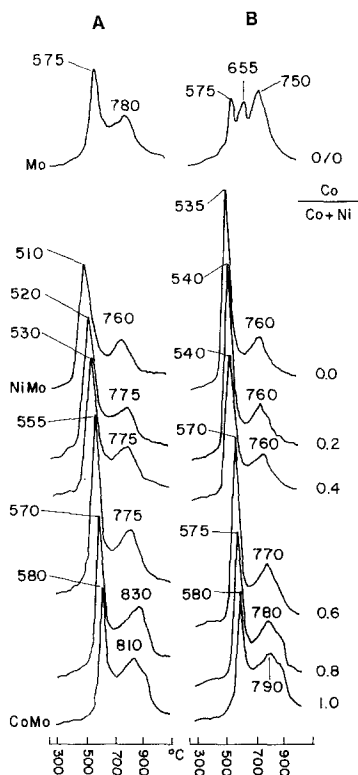


FIG. 3. TPR spectra of the oxide catalysts. Calcination at: (A) 500°C; (B) 600°C.

calcined at 600°C (not shown), and for other HDS catalysts studied previously (15, 19, 28).

Figure 6 shows that catalyst sulfidation produced a large increase in steady-state HDS activity, except in the case of the non-promoted samples. In general, there was not a significant effect of the calcination temperature on the activity of promoted catalysts. It is also seen that the Ni-promoted catalyst was more active than the Co-promoted one, either with or without presulfiding.

In contrast to previous works (20–22) using NiCo-Mo/Al₂O₃ that report optimum *r*-values producing maximum steady-state HDS activities, Figure 6 shows minimum activities for the present NiCo-Mo/SiO₂ catalysts. Note that Fig. 1 showed a similar trend in surface area suggesting that the observed minima in thiophene conversion could be merely a surface area effect. How-

ever, it is not clear that a small decrease in surface area, as shown in Fig. 1, could be the origin for the minimum in activity, since the areas are much in excess of a Mo monolayer.

DISCUSSION

Results on surface area and XRD (Figs. 1 and 2) suggest that molybdenum is captured by the promoter, through formation of a promoter molybdate hydrate, so that two deleterious effects, crystal growth by stacking of MoO₃ (010) planes and sintering of the silica support, are suppressed at 600°C.

Coincidentally, the presence of Ni promoter has been shown (25) to inhibit sintering resulting from the interaction of Mo with alumina during calcination. In that case, the formation of the sinterization product, Al₂(MoO₄)₃, was detected.

Taking into account the relatively high surface area of the silica gel employed in the present work as support (560 m²/g), it may be advanced that it was highly hydroxyl-

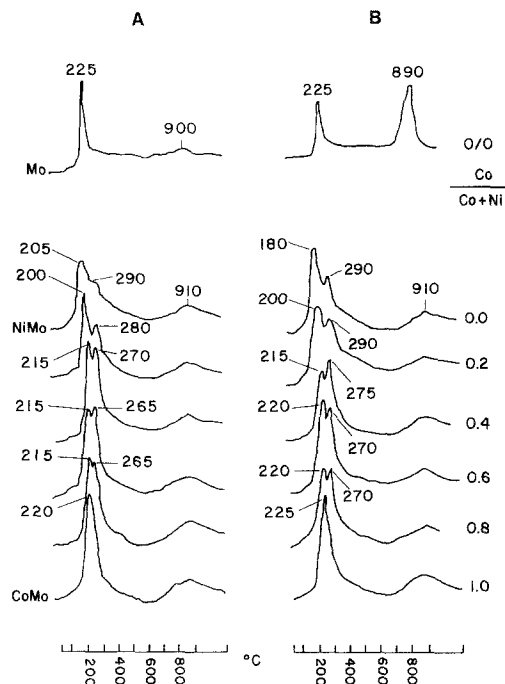


FIG. 4. TPR spectra of the presulfided catalysts. Calcination at: (A) 500°C; (B) 600°C.

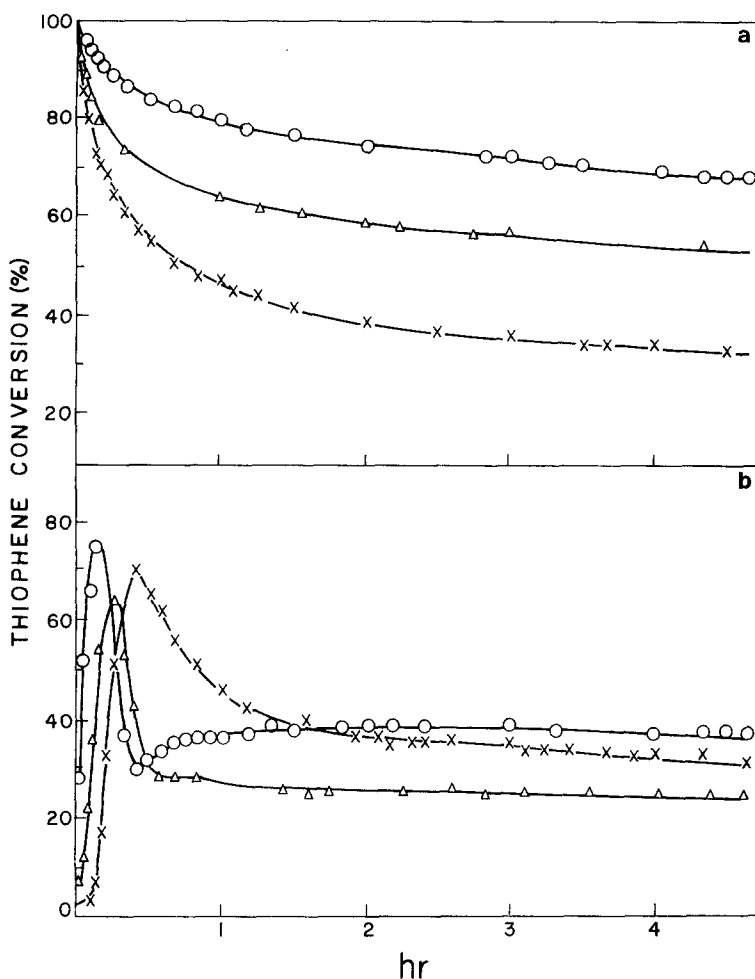


FIG. 5. Typical activity behavior (400°C). (a) with presulfidation (1-g samples); (b) nonpresulfiding (2-g samples). \times , $r = 0/0$; \circ , $r = 0.0$; Δ , $r = 1.0$.

ated. Sintering may proceed following dehydroxylation, by the collapse of the skeletal structure left after water evolution. Accordingly, if we assume that the Mo species were linked to the support by hydroxyl groups, sintering in the sample with $r = 0/0$ most likely occurred as a result of dehydroxylation assisted by a dislinking of molybdenum from the support after calcination at 600°C. Such phenomena probably involved decomposition of $\text{MoO}_2(\text{OH})_2$ (27) or of complex Mo-Si hydroxiphases to generate free MoO_3 and water vapor.

The presence of hydrated MoO_3 sup-

ported on silica has been suggested earlier (29, 30). This is apparently transformed to well-crystallized anhydrous MoO_3 after calcining at 600°C the 0/0 sample (Fig. 2). This is not the case of the promoted catalysts, where the hydrated state appears to be stabilized, within the range of T_c employed, through the formation of the hydrated promoter molybdate.

The anhydrous promoter molybdate is known not to be a good precursor phase for HDS (31, 32), and in contrast with present results, it has been detected elsewhere in samples prepared using another silica as

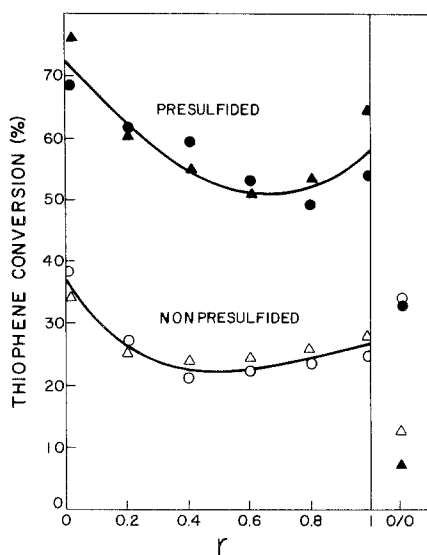


FIG. 6. Steady-state catalytic activities. Calcined at: \bullet , 500°C; \blacktriangle , 600°C. With presulfidation (1-g samples): solid symbols; nonpresulfiding (2-g samples): open symbols.

support (32). However, the surface area of that support was relatively low (179 m²/g) in comparison with the silica employed in present work (560 m²/g), suggesting less possibility of interaction of the species formed during calcination with surface hydroxyl groups to form the hydrated phase.

As a difference with the anhydrous phase, hydrated nickel molybdate has been reported to be an effective precursor phase for high activity sulfided catalyst (33). This was attributed to its easier sulfidability in comparison with the more refractory anhydrous nickel molybdate. The easier sulfidability of the hydrated state is probably associated with the positive effect of water vapor on sulfidability reported earlier (34). Accordingly, the presence of the promoter in the present series of catalysts seems to help in attaining a proper sulfidation, and hence high catalytic activity, through formation of a more sulfidable-hydrated phase.

The appearance of a TPR peak assigned to an oxidic phase difficult to sulfide (Fig. 4B, peak at 890°C in sample 0/0) is also in

accordance with the proposed enhancement of sulfidation effected by the promoter. This phase is probably MoO₂, formed during sulfidation from the anhydrous, well-crystallized MoO₃ (25, 34). However, MoO₂ was not clearly seen by XRD in sulfided samples, suggesting that it is amorphous, and probably a "porous" MoO₂ as reported by Arnoldy *et al.* earlier (35).

The easier sulfidability brought by the presence of the promoter can probably also be associated with the more rapid thiophene conversion increase observed when starting with initial nonpresulfided catalysts (Fig. 5b).

A comparison of present TPR results with previous ones (23, 26) using the same experimental conditions indicates the following order in first peak temperature: alumina-supported MoO₃, 480°C; silica-supported MoO₃ (present work), 575°C; and unsupported MoO₃, 725°C. This sequence suggests that a relation may exist between the temperature of the first TPR peak and the dispersion of the corresponding phase; i.e., lower temperature implies better dispersion. Confirming this relation, the previously studied series supported on alumina (20, 21) did not respond to XRD as the present series, even though the latter had larger surface area. A possible consequence of this is the fact that the present series of catalysts has activities representing reaction rates about four times smaller than those obtained previously for the series supported on alumina (21).

Another correspondence between TPR and XRD can be established in the sample with $r = 0/0$, where the marked sharpening of XRD signal resulting from increasing T_c from 500 to 600°C (Fig. 2) cannot be associated with a displacement of the first TPR peak (575°C, Fig. 3A) to a higher temperature, but with a splitting into two peaks (575 and 655°C, Fig. 3B). Accordingly, a general rule could be formulated stating that TPR peak-temperature displacement are the result of changes in dispersion, and that new peaks are assigned to new phases; therefore,

the appearance of the peak at 655°C is attributed to a different phase, one more crystalline and less connected to the support ("free" MoO₃) formed from the polymolybdates as indicated above.

Moreover, a comparison of the peak temperature attributed to MoO₂ between reduced (750–780°C, Fig. 3) and sulfided (890–900°C, Fig. 4) samples with $r = 0/0$ suggests a more dispersed MoO₂ in the first case.

The correlation between TPR and dispersion can also be established in promoted catalysts: the decrease or increase in first peak temperature in TPR of promoted oxide samples (Fig. 3) is accompanied by a respective broadening or sharpening of the XRD signal, corresponding to the hydrated promoter molybdate phase (Fig. 2), i.e., samples with $r = 0.0$ and 0.4 calcined at 500°C showed the broadest XRD signals at about $2\theta = 27^\circ$ and hence the lowest TPR signals (510–530°C). These latter increased to 535–540°C, with a corresponding sharpening in XRD signals after calcining at 600°C. On the other hand, the sample with $r = 1.0$ had both invariable TPR peak temperature (580°C) and invariable XRD signal sharpness for both T_c . The sample with $r = 0.6$ showed a correlation similar to $r = 1.0$. It can also be seen that samples with high r -values ($r = 0.6$ – 1.0) have both sharper XRD signals and larger first peak temperature than samples with low r -values ($r = 0.4$ – 0.0) for both T_c .

After sulfiding, there was practically no response to XRD suggesting a highly dispersed state. This correlates with the very low temperature of the first peak in the TPR spectra around 200°C (Fig. 4). Note that well-crystallized sulfide compounds give TPR spectra with much higher temperature: for example, pure MoS₂, NiS, and Ni₃S₂ produce TPR spectra with peak temperature well over 500°C (36).

Regarding the activity results, the larger extent of deactivation during use in HDS of nonpromoted samples as compared with

promoted catalysts (Fig. 5) reinforces previous reports that have attributed to the promoter a role associated with protecting the catalyst against initial deactivation (15–17). The referred protection seems to be accomplished better by Ni than by Co (Fig. 5). Indeed, NiMo catalysts have been found to inhibit carbon deposition better than CoMo (18), probably because of a better hydrogenation function of Ni.

The absence of a maximum in HDS activity for an intermediate r -value (Fig. 6) suggests that alumina is a necessary component for the occurrence of the dual promoting effect (i.e., the maximum) reported earlier (20–22). The stronger interaction of the supported species with alumina as compared with silica, referred to elsewhere (37), is probably an explanation for a better dispersant role cited above for alumina. This must be taken into account if the two opposed dual effects observed, i.e., the maximum and minimum, are to be investigated further.

CONCLUSIONS

The promoter dual effect (Co + Ni) on HDS activity can be strongly influenced by the type of support. Thus, a positive or a negative effect occurs when using alumina (20, 21) or silica (this work) respectively. The promoter (Ni or Co) may have a positive role in each of the steps of the catalyst history: inhibiting sintering of the support and MoO₃ crystal growth during calcination; providing an appropriate precursor phase (the hydrate) for catalyst sulfidation; and inhibiting initial catalyst deactivation during use in HDS reaction. Nickel-promoted catalyst can provide a more dispersed and reducible hydrate precursor phase and may be less prone to initial deactivation than cobalt-promoted catalyst.

ACKNOWLEDGMENTS

Support from the Consejo Nacional de Investigaciones Científicas y Tecnológicas is gratefully acknowledged. We also thank Oswaldo Carias for obtaining the XRD spectra.

REFERENCES

1. Gates, B. C., Katzer, J. R., and Schuit, G. C. A., "Chemistry of Catalytic Processes," p. 390. McGraw-Hill, New York, 1979.
2. Delmon, B., in "Proceedings, 3rd Climax Conference on Molybdenum" (H. F. Barry and P. C. H. Mitchell, Eds.), p. 33. Climax Co., Michigan, 1979.
3. Massoth, F. E., and Muralidhar, G., in "Proceedings, 4th Climax Conference on Molybdenum" (H. F. Barry and P. C. H. Mitchell, Eds.), p. 343. Climax Co., Michigan, 1982.
4. Topsoe, H., and Clausen, B. S., *Appl. Catal.* **25**, 273 (1986).
5. Prins, R., de Beer, V. H. J., and Somorjai, G. A., *Catal. Rev.-Sci. Eng.* **31**, 1 (1989).
6. Topsoe, H., Clausen, B. S., Candia, R., Wivel, C., and Morup, S., *Bull. Soc. Chim. Belg.* **90**, 1189 (1981).
7. Hagenbach, G., Courty, P. H., and Delmon, B., *J. Catal.* **31**, 264 (1973).
8. Hayden, T. F., and Dumesic, J. A., *J. Catal.* **103**, 366 (1987).
9. Roxlo, C. B., Daage, M., Ruppert, A. F., and Chianelli, R. R., *J. Catal.* **100**, 176 (1987).
10. Derouane, E. G., Pendersen, E., Clausen, B. S., Gabelica, Z., Candia, R., and Topsoe, H., *J. Catal.* **99**, 253 (1986).
11. Harris, S., and Chianelli, R. R., *J. Catal.* **98**, 17 (1986).
12. de Beer, V. H. J., Duchet, J. C., and Prins, R., *J. Catal.* **72**, 369 (1981).
13. Burch, R., and Collins, A., *J. Catal.* **97**, 385 (1986).
14. Ledoux, M. J., Michaux, O., Agostini, G., and Panissod, P., *J. Catal.* **96**, 201 (1985).
15. Laine, J., Brito, J., Gallardo, J., and Severino, F., *J. Catal.* **91**, 64 (1985).
16. Laine, J., Brito, J., and Severino, F., *Appl. Catal.* **15**, 333 (1985).
17. Yitzhaki, D., and Aharoni, C., *J. Catal.* **107**, 255 (1987).
18. Laine, J., Brito, J., and González, R., in "Proceedings, 4th Climax Conference on Molybdenum" (H. F. Barry and P. C. H. Mitchell, Eds.), p. 358. Climax Co., Michigan, 1982.
19. Laine, J., Severino, F., and Golding, R., *J. Chem. Tech. Biotechnol.* **33A**, 387 (1984).
20. Cáceres, C., Fierro, J. L. G., López-Agudo, A., Severino, F., and Laine, J., *J. Catal.* **97**, 219 (1986).
21. López-Agudo, A., Fierro, J. L. G., Cáceres, C., Laine, J., and Severino, F., *Appl. Catal.* **30**, 185 (1987).
22. Laine, J., Severino, F., Cáceres, C., Fierro, J. L. G., and Lopez Agudo, A., *J. Catal.* **103**, 228 (1987).
23. Brito, J., and Laine, J., *Polyhedron* **5**, 179 (1986).
24. Laine, J., Pratt, K. C., and Trimm, D. L., *Ind. Eng. Chem. Prod. Res. Dev.* **18**, 329 (1979).
25. Laine, J., and Pratt, K. C., *Ind. Eng. Chem. Fundam.* **20**, 1 (1981).
26. Brito, J. L., Laine, J., and Pratt, K. C., *J. Mater. Sci.* **24**, 425 (1989).
27. Seyedmonir, S. R., Abdo, S., and Howe, R. F., *J. Phys. Chem.* **86**, 1233 (1982).
28. Massoth, F. E., and Kibby, C. L., *J. Catal.* **47**, 300 (1977).
29. Sonnemans, J., and Mars, P., *J. Catal.* **31**, 209 (1973).
30. Marcinkowka, K., Rodrigo, L., Kaliaguine, S., and Roberge, P. C., *J. Catal.* **97**, 75 (1986).
31. Gajardo, P., Grange, P., and Delmon, B., *J. Phys. Chem.* **83**, 1771 (1979).
32. Gajardo, P., Pirotte, D., Grange, P., and Delmon, B., *J. Phys. Chem.* **83**, 1780 (1979).
33. Laine, J., and Pratt, K. C., *React. Kinet. Catal. Lett.* **10**, 207 (1979).
34. Arnoldy, P., Van den Haijkant, J. A. M., de Bock, G. D., and Moulijn, J. A., *J. Catal.* **92**, 35 (1985).
35. Arnoldy, P., de Jonge, J. C. M., and Moulijn, J. A., *J. Phys. Chem.* **89**, 4517 (1985).
36. Brito, J., and Laine, J., unpublished results.
37. Laine, J., Yunes, S., Brito, J., and Andreu, P., *J. Catal.* **62**, 157 (1980).